Synthesis and characterization of La_2NiMnO_6 nanoparticles at low temperature

P. S. R. Murthy[a], Ciano Fernandes[a], Shubham Gaonkar[a], Samruddhi Azrekar[a], Apoorba Singh[a]

[a]Dhempe College of Arts and Science, Goa, India.

ABSTRACT

The synthesis, structure and characterization of La_2NiMnO_6 nanoparticles were studied using a simple sol-gel combustion method at 600°C. The overall process involves three steps – formation of homogenous solution, formation of dried gel and final combustion of the dried gel. On ignition in air, the compound is found to transform into nanosized La_2NiMnO_6 nanoparticles. The analysis of X-ray diffraction (XRD) data confirmed the monoclinic La_2NiMnO_6 perovskite of space group $P2_{1/n}$ without any impurity phase. The Scherrer's formula was employed to estimate the crystallite size of the prepared sample. For a further insight into the crystal structure, Scanning electron microscopy (SEM) imaging was done. The estimated values of the crystallite size from Scherrer's formula and SEM were found to be roughly the same. The SEM images confirmed the polycrystalline nature of the prepared sample. Furthermore, UV measurements were performed on the compound to estimate its band gap energy. The values were found to match well with those reported elsewhere in literature. EDX measurements performed on the sample confirmed the existence of La, Ni, Mn and O elements.

KEYWORDS: *Auto-combustion, Rietveld refinement, nanoparticles, orthorhombic, diffuse reflectance.*

I. INTRODUCTION

Perovskite oxides are studied widely for their uniqueness in structural, magnetic, optical and electrical properties. Similarly, double perovskites with the general chemical formula $A_2BB'O_6$ have gained popularity, where A is an alkaline earth or rare earth element and B & B' are 3d transition metals [1]. Among the double perovsites, La based compounds have received wider attention due to their different structural, magnetic and electrical properties [2, 3, 4]. In the La_2NiMnO_6 double perovskite, herein referred to as LNMO, La^{3+} with an ionic radius (1.06A°) occupies position A of the complex perovskite structure, whereas Ni^{3+} with an ionic radius(0.66A°) and Mn^{3+} with an ionic radius (0.55A°) cations occupy the B and B' positions, respectively. The presence of La^{3+}, Ni^{3+} and Mn^{3+} ions make the compound structurally stable and magnetically interesting with its complex magnetic ordering. The different types of magnetic ordering encountered in the LNMO compound is based on different preparation techniques employed [3, 4, 5-8].

The individual properties of B and B' cations of double perovskite compounds play a key role in determining the structural, optical, magnetic and electronic properties. Among the double perovksites, La based compounds have received wide attention due to their different structural, magnetic and electrical properties. The double perovskite LNMO with band gap energy of 1.5 eV was reported by Kitamura et al [14]. The LNMO can be synthesized by a chemical method which is a much easier method than the methods to prepare double perovsites. Different crystal structures have been found to form at different synthesis conditions that influence the physical properties of LNMO such as band gap and magnetic properties. Hence, here, in this work, an attempt has been made to synthesize LNMO using a simple sol-gel technique at a much lower temperature. Therefore, this paper presents an interesting opportunity for further analysis of LNMO.

II. EXPERIMENTAL

La_2NiMnO_6 was prepared using a citrate-nitrate auto-combustion method. Analytical grade La $(NO_3)_2.6H_2O$, Ni $(NO_3)_2.6H_2O$ and Mn $(CH_3COO)_2.4H_2O$ were used as starting materials. The starting materials were discretely dissolved in distilled water and then mixed together under constant stirring at 70°C. Citric acid was added to the mixture as fuel and the pH of the solution was controlled by drop-wise adding of proper amount of ammonia solution during the stirring process as so maintain the pH = 7. Ethylene glycol was then added to the mixture and heated at about 200°C in open air by decomposing the dried gel and finally a dark brown powder was formed after an intense exothermic combustion reaction. The powder was ground and then

---

calcined at 600°C for three hours followed by pelletization and sintering at 600°C for five hours. Nanocrystalline LNMO was obtained.

The sample was deemed to be phase pure, as X-ray diffraction recorded (XRD) data collected on a Rigaku X-ray diffractometer in the range of $10° \leq \Theta \leq 80°$ using CuK_α (λ =1.5418 A°) radiation showed no impurity reflections. The diffraction patterns was Rietveld refined using FULLPROF suite and structural parameters were obtained. UV-visible diffuse reflectance spectra were recorded for the sample in the range of 200 to 800 nm at the Department of Physics, Goa University. Scanning electron microscope (SEM) image and Energy dispersive X-ray spectrometer were recorded on the Zeiss make scanning electron microscope at the Instrumentation Centre, Goa University.

III. RESULTS AND DISCUSSION

Fig. 1 shows the room temperature Rietveld refined XRD pattern of the gel combustion synthesized LNMO powder prepared by the citrate-nitrate auto-combustion technique. The XRD pattern confirms the formation of a pure LNMO phase with a well-defined monoclinic structure in the space group SG $P2_{1/n}$, without any impurity phase. The obtained lattice parameters, atomic positions, bond lengths and the bond angles shown in table 1 are in good agreement with those reported in literature [13]. The sample was synthesized at 600°C and dark brown in colour. The XRD pattern has a peak at around 32° which suggest that the crystallization is monoclinic in the space group $P2_{1/n}$. This is found to be in close agreement with that reported [15] wherein the sample was annealed at 900°C in oxygen atmosphere. Earlier reports have indicated that the crystallization of LNMO into the Pnma space-group, having orthorhombic symmetry and the cubic Pm-3m structure. The monoclinic structure reported here might be due to the synthesis methodology and the sintering temperature involved.
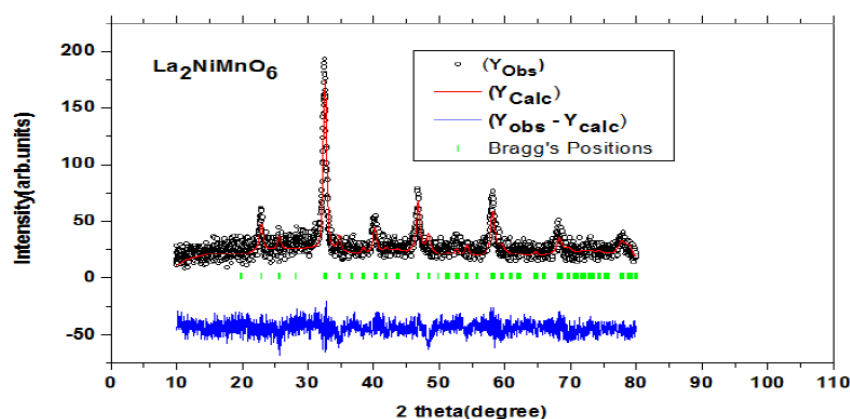

Fig. 1. *Rietveld refined XRD data of LNMO. The open circles (black) show the observed counts, the continuous line (red) passing through these counts is the calculated profile and the difference between the observed and calculated patterns (blue) is shown as a continuous line at the bottom of the two profiles. The Bragg positions (green) are shown as vertical bars.*

The FULLPROF program was used for Rietveld analysis of the XRD data for LNMO. Refinements were performed in the space group $P2_{1/n}$. In each refinement, a total of more than twenty parameters were refined: zero shift, scale factor, background coefficients, lattice parameters, asymmetric parameters, oxygen parameters for isotropic temperature factor and full width at half maximum. The Rietveld plot for the prepared LFMO is shown in Fig. 1 above. The observed intensity data are plotted in the upper section as points (black). The calculated intensities are shown in the same section as curves (red). The difference between the observed and calculated intensities is shown in the lower section (blue). The short vertical bars in the centre of the plot show the Bragg positions (green). Rietveld refinement of the data results in a B-site ordered monoclinic structure with the $P2_{1/n}$ space group. The obtained lattice parameters, atomic positions are consistent with those reported in literature [13]. Atomic coordinates for each cation in the A and B sites, the residual errors and the refined lattice parameters for the monoclinic LNMO perovskite with space group $P2_{1/n}$ is displayed in table 1.

Label	Type	Atomic coordinates			B_{iso}	Occupancy
		x	y	z		
La	La	-0.00126	0.01855	0.25520	0.40000	0.62710
Ni	Ni	0	0.5	0	0.40000	0.25163
Mn	Mn	0.5	0	0	1.16834	0.33031
O1	O	0.04400	0.49480	0.24490	18.0589	1.0
O2	O	0.74200	0.28100	0.01130	1.14069	1.0

O3	O	0.29500	0.70000	0.53000	1.14069	1.0

$\alpha = \gamma = 90°$, $\beta = 89.4°$			
a/A°	5.5139	R_{exp}	1.88
b/A°	5.4600	R_{wp}	6.16%
c/A°	7.7399	R_p	5.26%
V/A°	246.18	χ	1.06
a/b	1.0098	R-factor	1.75%
c/b	1.4175	RF-factor	1.56%

Table 1: Atomic coordinates for each cation in the A and B sites, R factors, equivalent thermal parameters and refined lattice parameters for the monoclinic LNMO perovskite with space group P2$_{1/n}$.

The crystalline size of the LNMO sample as seen in Fig.2 was calculated by the X-ray line broadening method using the Scherrer's formula $D = k\lambda/\beta\cos\Theta$, where D is the crystallite size in nanometers, λ is the beam wavelength (λ = 1.5414 A°), k is a constant equal to 0.94, β is the integral breadth and Θ is the peak position.. The average crystalline size is calculated to be about 27.8 nm.
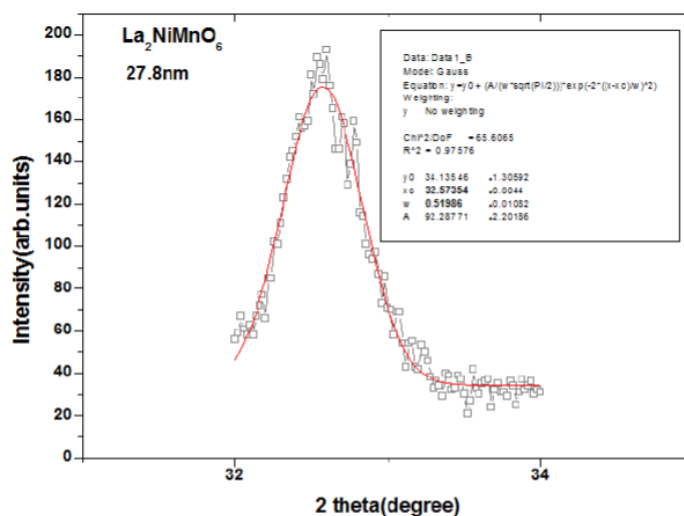

Fig.2. *Gaussian fit to the XRD data for determining the particle size of LNMO.*

For semiconductor materials, the energy bandgap can be determined by their optical absorption performance. The UV-visible diffuse reflectance spectra of the LNMO nanoparticles in terms of absorbance were collected as a function of the wavelength in nm. The optical bandgap of the LNMO nanoparticles can be deduced from the spectra by determining the cut-off wavelength λ_c. Fig. 3 indicates the bandgap of LNMO to be 1.7 eV. This is similar to that of the single perovskite LaMnO₃ whose experimental band gap is 1.7 eV and the theoretical band gap is 2.0 eV [16]. This can be attributed to a very small distortion of LNMO crystalline after the introduction of Ni³⁺ in to the B-site [17].Reported values of band gap in the rhombohedral phase are 1.4eV and in the monoclinic phase is 1.2 eV [15]. The difference in the bandgap values can be attributed to a larger distortion of the B-site in the reported rhombohedral phase then in the monoclinic phase and a lower annealing temperature.
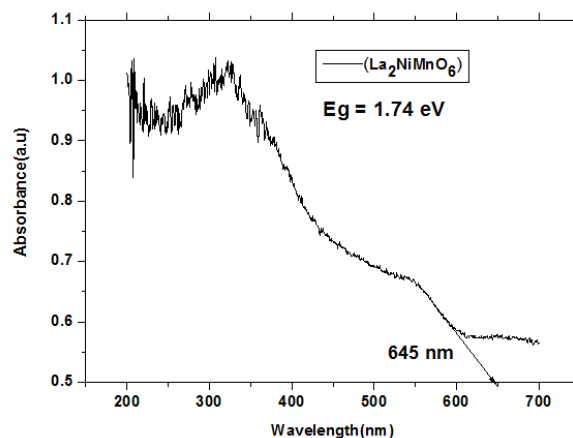

Fig.3. *UV visible spectra for LNMO.*

SEM was employed to obtain direct information about the size and structure of the produced LNMO nanocrystals. Fig. 4 presents a typical SEM image. It can be seen that homogenous nanoparticles are formed in the sample. The average particle size is about 26.3 nm; a smaller particle size can be attributed to a lower synthesizing temperature. Particle agglomeration is also observed due to lower annealing temperature of 600°C.
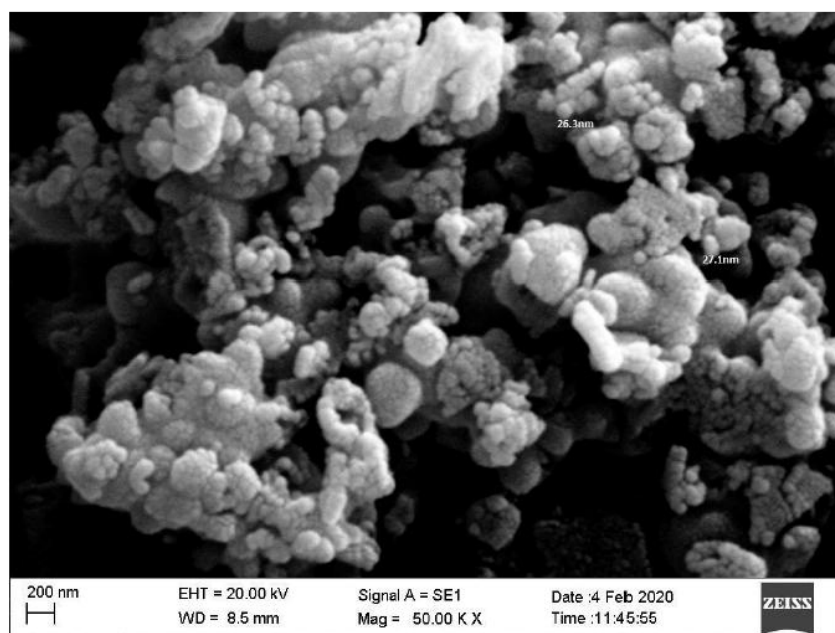

Fig. 4. *SEM measurements for LNMO with a particle size of 26.3 nm at 50K magnification.*

Energy dispersive X-ray was performed on the LNMO sample to confirm the sample composition. Three different areas were arbitrarily selected to ascertain the sample composition. The EDX results from the sample as seen in Fig. 5 confirm the existence of La, Ni and Mn elements. The spectra are similar to that reported in [15]. The stoichiometric ratio of Mn and Ni in the prepared product is approximately 1:1 as seen in Table 2.
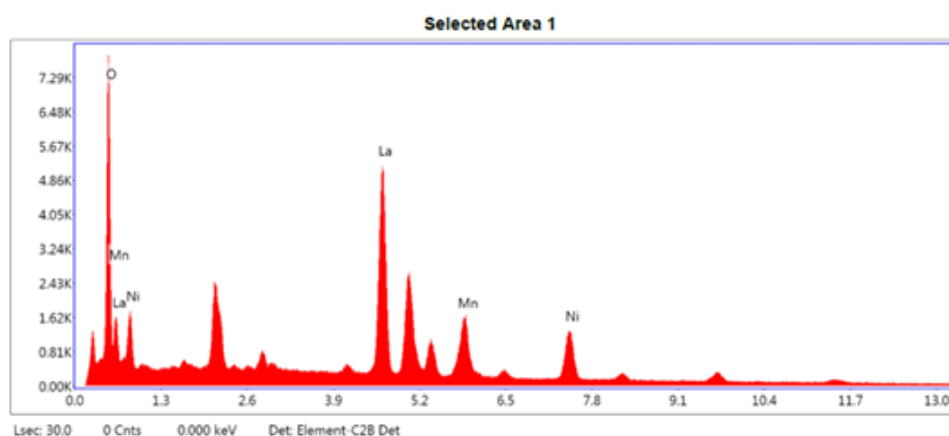

Fig. 5. *EDX pattern for LNMO (La₂NiMnO₆)*

Table 2: Stoichiometric ratio of La, Ni, Mn and O

Element	O-K	Mn-K	Ni-K	La-L
Wt%	15.41	11.49	15.36	57.74
Atom %	52.07	11.31	12.34	24.28

IV. CONCLUSION

In summary, the synthesis, characterization, composition and band gap energy were studied at a low temperature of 600°C using a simple sol-gel technique. Nanosized La$_2$NiMnO$_6$ powders of 27.8 nm particle size were prepared directly through the simple sol-gel auto-combustion technique. The entire process of synthesizing pure nanosized La$_2$NiMnO$_6$ powders involves three steps: formation of solutions, formation of the dried gel in air followed by auto-combustion that can be considered as a heated-induced exothermic oxidation-reduction reaction between the nitrate and carboxyl groups. The process is easy, simple and cost effective although analytical grade compounds were used as starting materials. The XRD pattern confirmed the formation of a pure LNMO phase with a well-defined monoclinic structure in the space group P2$_{1/n}$, without any impurity phase. The crystalline size of the LNMO sample was calculated by the X-ray line broadening method using the Scherrer's formula and average crystalline size is calculated to be about 27.8 nm. UV measurements performed on the powders reveal band gap energy of about 1.7 eV. SEM measurements indicate particles with an average size of 26.3 nm, which is consistent with the size obtained from the peak broadening in X-ray diffraction studied of LNMO. Such a consistency implies that the LNMO nanoparticles are polycrystalline. EDX measurements performed on the powders are a clear confirmation of the existence of La, Ni, Mn and O elements.

ACKNOWLEDGEMENT

REFERENCES

[1]. M.Dhilip, N. Aparna Devi, J. stella Punitha, V. Anbarasu, K. saravana Kumar ,Vaccum 167 (2019) 16-20.
[2]. W. Wang,W.Feng, J. Yuan, Phys. B. Condens. Matter 540 (2018) 33.
[3]. D. Yang,T.Yang, P. Mukherjee, D. Huo, SE Dutton, M.A Carpenter, Phys. Rev. B 99 (2019).
[4]. P.M. Tirmali, D.K. Mishra, B.P. Benglorkar, S.M.Mane, S.L. Kadam, S.B. Kulkarni, Journal of the Chinese Advanced Materials Society 6 (2016) 207.
[5]. Petrucio Barrozo, N.O. Moreno and J. Albina Aguiar. Adv.Mater. Res. 975 (2014) 122-127.
[6]. R. Shaheen ,J. Bashir, M. Siddique, H. Rundlöf, A. R.Rennie, Phys. B. Condens. Matter 385-386 (2006) 103.
[7]. K. Ramesha , V.Thangadurai, D.Sutar. S.V. Subramanyam, G.N. Subbanna, J. Gopalkrishnan, Mater. Res. Bull. 35(2000) 559.
[8]. R. C. Sahoo , S.Das, T.K. Nath, J. Magn. Magn. Mater. 460 (2018) 409.
[9]. *O′Keefe, M., & Hyde, B.G. (1977). Acta Cryst. B33, 3802-3813.*
[10]. Jasnamol P P,P. Neenu :akshmi, Senoy Thomas, K. G. Suresh, Manoj Raama Varma, RSC Advances, DOI: 10.1039C5RA24092A.
[11]. K.Rida, M.A. Ṕena, E. Sastre,A. Martinez-Arias, Journal of Rare Earths, Vol. 30, No.3, Mar. 2012, P.210.
[12]. N.Özbay and R.Z. Yarbay Şahin ,AIP Conf.Proc.1809, 020040-1-020040-9;doi:10.1063/1.4975455.
[13]. K.Devi Chandrasekhar, A.K. Das, C.Mitra ,A. Venimadhav J. Phys. Condens. Matter, 24 (2012) 495901.
[14]. M. Kitamura, I. Ohkubo, *M*. Kubota, Y. Matsumoto, H. Koinuma, and *M*. Oshima, *Appl. Phys*. Appl. Phys. Lett., 94 (2009) 262503.
[15]. Chunfeng Lan, shuai Zhao, Tingting Xu, Jie Ma, Shuzi Hayase, Tingli Ma, Journal of Alloys and Compounds, 655 (2016) 208-214.
[16]. D. Munoz, N.M. Harrison, F. Illas, Phys. Rev. B (69) 2004 085115.
[17]. M.C. Sánchez,J. Garcia,J. Blasco, G.Subias, J-Perez-Cacho, Phys. Rev. B (65) 2002 144409.